Inorganic Chemistry

ARTICLE

pubs.acs.org/IC

En Route to Osmium Analogues of KP1019: Synthesis, Structure, Spectroscopic Properties and Antiproliferative Activity of *trans*-[$Os^{IV}Cl_4$(Hazole)$_2$]

Gabriel E. Büchel, Iryna N. Stepanenko, Michaela Hejl, Michael A. Jakupec, Bernhard K. Keppler, and Vladimir B. Arion*

University of Vienna, Institute of Inorganic Chemistry, Währinger Strasse 42, A-1090 Vienna, Austria

Supporting Information

ABSTRACT:

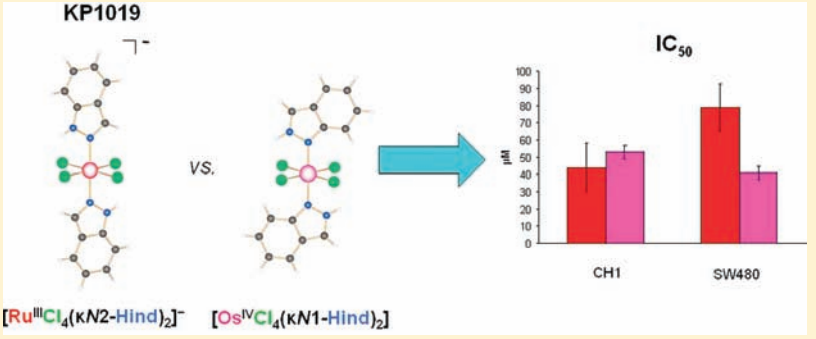

By controlled Anderson type rearrangement reactions complexes of the general formula *trans*-[$Os^{IV}Cl_4$(Hazole)$_2$], where Hazole = 1*H*-pyrazole, 2*H*-indazole, 1*H*-imidazole, and 1*H*-benzimidazole, have been synthesized. Note that 2*H*-indazole tautomer stabilization in *trans*-[$Os^{IV}Cl_4$(2*H*-indazole)$_2$] is unprecedented in coordination chemistry of indazole. The metal ion in these compounds possesses the same coordination environment as ruthenium(III) in (H_2ind)[$Ru^{III}Cl_4$(Hind)$_2$], where Hind = 1*H*-indazole, (KP1019), an investigational anticancer drug in phase I clinical trials. These osmium(IV) complexes are appropriate precursors for the synthesis of osmium(III) analogues of KP1019. In addition the formation of an adduct of *trans*-[$Os^{IV}Cl_4$(Hpz)$_2$] with cucurbit[7]uril is described. The compounds have been comprehensively characterized by elemental analysis, EI and ESI mass spectrometry, spectroscopy (IR, UV−vis, 1D and 2D NMR), cyclic voltammetry, and X-ray crystallography. Their antiproliferative acitivity in the human cancer cell lines CH1 (ovarian carcinoma), A549 (nonsmall cell lung carcinoma), and SW480 (colon carcinoma) is reported.

INTRODUCTION

In the past six years several research groups reported on the synthesis and screening for antiproliferative activity in vitro of osmium coordination compounds and osmium(II)-arene species,[1−3] as well as on studies of their reactivity with DNA model compounds.[4] These investigations showed that osmium is another metal that deserves attention for the development of effective inorganic antitumor drugs. Osmium analogues that are equipotent to their ruthenium congeners have the advantage of being more inert under conditions relevant for drug formulation.[2c] Of particular academic interest are also the observed or established differences between ruthenium and osmium compounds in stabilization of higher oxidation states, magnitude of spin−orbit coupling, metal−ligand exchange reactions, and so forth.[5−8]

In pursuing the goal of establishing structure-cytotoxicity relationships for osmium-azole-chlorido series and creating active metal-based antitumor drugs, we already reported the synthesis of *trans*-[$Os^{III}Cl_2$(Hazole)$_4$]Cl, *cis*-[$Os^{III}Cl_2$(Him)$_4$]Cl, and *mer*-[$Os^{III}Cl_3$(Hazole)$_3$].[3b,9,10] Compounds of the last type were insoluble in water, rendering tests for antiproliferative activity in vitro impossible, while *trans*-[$Os^{III}Cl_2$(Hazole)$_4$]Cl showed noteworthy antiproliferative effects in the cell lines A549 (nonsmall cell lung cancer), CH1 (ovarian carcinoma), and SW480 (colon carcinoma), with IC_{50} values in the 10^{-6} to 10^{-5} M concentration range.[3b] *trans*-[$Os^{III}Cl_2$(Hpz)$_4$]Cl was found to be more active than the ruthenium counterpart, whereas the osmium(III) imidazole complex was less cytotoxic than the ruthenium analogue in all three cell lines.

Quite recently, Anderson type rearrangement reactions[11] of (H_2azole)$_2$[$Os^{IV}Cl_6$] in alcohols in the presence of tetrabutylammonium chloride enabled the synthesis of the next family of compounds, namely, (n-Bu_4N)[$Os^{IV}Cl_5$(Hazole)], where Hazole = 1*H*-pyrazole, 1*H*-indazole, 1*H*-imidazole, 1*H*-benzimidazole, or 1*H*,2,4-triazole.[5] The (n-Bu_4N)$^+$ was also substituted

Received: April 8, 2011
Published: July 08, 2011

Chart 1. Compounds Reported in This Work[a]

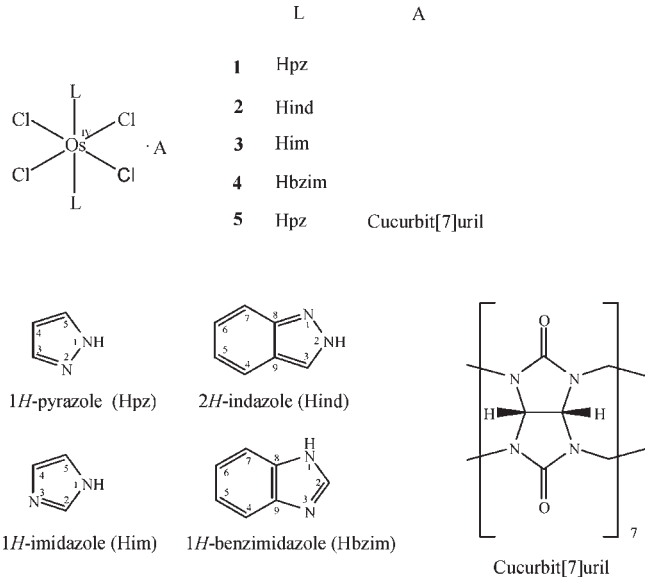

[a]All complexes have been characterized by X-ray crystallography; atom labeling was introduced for assignments of resonances in NMR spectra.

by biologically relevant or nontoxic cations such as Na^+ and $(H_2azole)^+$. Comparison of these osmium complexes with related ruthenium analogues, such as $(H_2azole)_2[Ru^{III}Cl_5(Hazole)]$ [12−15] and $(H_2azole)[Ru^{III}Cl_4(Hazole)_2]$[14] showed a clear preference for higher oxidation states of the heavier congener. The efficacy of the observed transformation is dependent on the electron-donating potency of the azole heterocycle and the solvent used. A deeper substitution at osmium(IV) was first observed in the case of imidazole and benzimidazole ligands with highest basicity and further investigated for other azole heterocycles.

In this paper, we report on the synthesis, X-ray diffraction studies, and spectroscopic characterization of osmium(IV) complexes, namely, *trans*-$[Os^{IV}Cl_4(Hazole)_2]$, where Hazole = 1*H*-pyrazole, 2*H*-indazole, 1*H*-imidazole, and 1*H*-benzimidazole. Of these compounds the osmium indazole complex is the first example in which the ortho-quinoid tautomer is stabilized upon coordination to the transition metal ion. The cytotoxic activity of all complexes has been assessed in three human cancer cell lines originating from different solid malignancies, namely, CH1 (ovarian carcinoma), A549 (nonsmall cell lung carcinoma), and SW480 (colon carcinoma). In addition, attempts to encapsulate the complexes prepared into the macrocyclic host molecule cucurbit[7]uril are also described (Chart 1).

EXPERIMENTAL SECTION

Materials. The starting compounds $[(DMSO)_2H]_2[OsCl_6]$ and $(H_2azole)_2[OsCl_6]$ (Hazole = Hpz, Him, Hind, Hbzim) were synthesized as previously reported in the literature.[3b,16,17] OsO_4 (99.8%) and $N_2H_4 \cdot 2HCl$ were purchased from Johnson Matthey and Fluka, respectively. 1*H*-Pyrazole, 1*H*-indazole, 1*H*-imidazole, 1*H*-benzimidazole, and 1-hexanol were from Aldrich and Fluka. All these chemicals were used without further purification. *trans*-$[OsCl_4(Hazole)_2]$ (Hazole = Hpz, Him, Hbzim) complexes were prepared under argon atmosphere using standard Schlenk techniques. The synthesis of *trans*-$[OsCl_4(2H\text{-ind})_2]$ was performed in the solid state in an evacuated glass oven. Cucurbit-[7]uril was generously offered by Marcel Wieland, Institute of Organic Chemistry, University of Vienna.

trans-[OsCl$_4$(Hpz)$_2$] (**1**). A suspension of $(H_2pz)_2[OsCl_6]$ (100 mg, 0.18 mmol) in 1-hexanol (2 mL) was stirred at 160 °C for 2 h. The red precipitate formed was filtered off, washed with ethanol and dried in vacuo. Yield: 40 mg, 47%. Anal. Calcd for $C_6H_8Cl_4N_4Os \cdot 0.1C_2H_5OH$ (M_r = 472.80 g/mol): C, 15.75; H, 1.83; N, 11.85. Found: C, 15.99; H, 1.59; N, 11.53. ESI-MS in MeOH (negative): *m*/*z* 332 $[OsCl_4]^-$, 467 $[OsCl_4(Hpz)_2-H]^-$, ESI-MS in MeOH (positive): *m*/*z* 491 $[OsCl_4(Hpz)_2+Na]^+$, 513 $[OsCl_4(Hpz)_2+2Na-H]^+$. EI-MS (positive): *m*/*z* 192 $[Os]^+$, 329 $[OsCl_2(Hpz)]^+$, 364 $[OsCl_3(Hpz)]^+$, 432 $[OsCl_3(Hpz)_2]^+$, 467 $[OsCl_4(Hpz)_2]^{+\bullet}$. MIR, cm^{-1}: 570, 593, 529, 662, 775, 904, 1052, 1072, 1113, 1165, 1263, 1345, 1398, 1482, 1507, 2014, 2166, 2363, and 3331. FIR, cm^{-1}: 159, 178, 265, 287, 325, 345, 571. UV−vis (MeOH), λ_{max}, nm (ε, M^{-1} cm^{-1}): 215 (11884), 245 (5 898), 277 sh (2578), 350 sh (4796), 382 (7981). UV−vis (DMSO), λ_{max}, nm (ε, M^{-1} cm^{-1}): 350 sh (5576), 385 (8404). ^1H NMR (DMSO-d_6, 500.32 MHz): δ −5.59 (d, 1H, J = 2.40 Hz, H_3), −2.97 (s, 1H, H_5), 6.48 (brs, 1H, H_4), 19.21 (s, 1H, H_1) ppm. $^{13}C\{^1H\}$ NMR (DMSO-d_6, 125.81 MHz): δ 73.52 (C_4), 181.14 (C_5), 218.41 (C_3) ppm. ^{15}N NMR (DMSO-d_6, 50.69 MHz): δ 115.5 (N_1) ppm. Suitable crystals for X-ray diffraction study were grown from a solution of **1** in acetone.

trans-[OsCl$_4$(κN$_1$-2H-ind)$_2$] (**2**). $(H_2ind)_2[OsCl_6]$ (166 mg, 0.25 mmol) was heated in the solid state at 150 °C in a glass oven for 45 h. The black product was extracted with methanol in a Soxhlet extractor for 24 h. The dark blue residue collected as a solid from the extraction thimble was recrystallized from dimethylformamide (DMF). Yield: 28 mg, 19%. Anal. Calcd for $C_{14}H_{12}Cl_4N_4Os$ (M_r = 568.31 g/mol): C, 29.59; H, 2.13; N, 9.86. Found: C, 29.52; H, 2.14; N, 9.52. ESI-MS in MeOH (negative): *m*/*z* 567 $[OsCl_4(Hind)_2-H]^-$. MIR, cm^{-1}: 591, 626, 734, 752, 838, 863, 895, 980, 1084, 1131, 1174, 1234, 1314, 1362, 1387, 1440, 1485, 1511, 1620, 1665, 3108, and 3346. FIR, cm^{-1}: 157, 181, 194, 217, 249, 262, 310, 324, 334, 429, 459, 550, 595, and 627. UV−vis (DMF), λ_{max}, nm (ε, M^{-1} cm^{-1}): 283 (9539), 362 (9194), 459 sh (2342), 491 (2767), 628 (12055). UV−vis (DMSO), λ_{max}, nm (ε, M^{-1} cm^{-1}): 265 (9658), 289 (9025), 369 (7785), 619 (12978). ^1H NMR (DMSO-d_6, 500.32 MHz): δ −4.44 (s, 1H), −3.28 (s, 1H), 0.58 (d, 1H, J = 8.51 Hz), 5.18 (s, 1H), 13.68 (s, 1H) ppm. Suitable crystals for X-ray diffraction study were grown from a solution of **2** in DMF.

trans-[OsCl$_4$(Him)$_2$] (**3**). A suspension of $(H_2im)_2[OsCl_6]$ (100 mg, 0.18 mmol) in 1-hexanol (2 mL) was stirred at 160 °C for 6 h. The brown precipitate formed was filtered off, washed with methanol and diethyl ether, and dried in vacuo. Yield: 37 mg, 44%. Anal. Calcd for $C_6H_8Cl_4N_4Os$ (M_r = 468.20 g/mol): C, 15.39; H, 1.72; N, 11.97. Found: C, 15.70; H, 1.56; N, 11.65. ESI-MS in MeOH (negative): *m*/*z* 468 $[OsCl_4(Him)_2-H]^-$, 934 $[\{OsCl_4(Him)\}_2-H]^-$, ESI-MS in MeOH (positive): *m*/*z* 490 $[OsCl_4(Him)_2+Na]^+$, 956 $[\{OsCl_4(Him)_2\}_2+Na]^+$. MIR, cm^{-1}: 584, 604, 641, 682, 738, 830, 1065, 1119, 1503, 2041, 2351, and 3359. FIR, cm^{-1}: 147, 178, 271, 281, 316, 343, 605, 643. UV−vis (MeOH), λ_{max}, nm (ε, M^{-1} cm^{-1}): 251 sh (2696), 280 (1967), 343 (5838), 374 (6458), 452 (1011). UV−vis (DMSO), λ_{max}, nm (ε, M^{-1} cm^{-1}): 344 (7209), 374 (7045), 450 sh (1422). ^1H NMR (DMSO-d_6, 500.32 MHz): δ −0.51 (s, 1H), 7.29 (s, 1H), 7.86 (s, 1H), 12.29 (s, 1H_1) ppm. $^{13}C\{^1H\}$ NMR (DMSO-d_6, 125.81 MHz): δ 119.52 {7.29}, 114.45 {7.86}, 188.36 {−0.51} ppm. ^{15}N NMR (DMSO-d_6, 50.69 MHz): δ 157.08 (N_1) ppm. Suitable crystals of **3**·2DMSO for X-ray diffraction study were grown from a solution of **3** in dimethylsulfoxide (DMSO).

trans-[OsCl$_4$(Hbzim)$_2$] (**4**). A suspension of $(H_2bzim)_2[OsCl_6]$ (200 mg, 0.31 mmol) in 1-hexanol (3 mL) was stirred at 160 °C for 8 h. The blue precipitate formed was filtered off, washed with methanol and diethyl ether, and dried in vacuo. Yield: 146 mg, 82%. Anal. Calcd for $C_{14}H_{12}Cl_4N_4Os$ (M_r = 568.31 g/mol): C, 29.59; H, 2.13; N, 9.86.

dx.doi.org/10.1021/ic200728b |*Inorg. Chem.* 2011, 50, 7690–7697

Table 1. Crystal Data and Details of Data Collection for 1, 2, 3·2DMSO, 4, and 5·11.25H_2O

	1	2	3·2DMSO	4	5·11.25H_2O
empirical formula	$C_6H_8Cl_4N_4Os$	$C_{14}H_{12}Cl_4N_4Os$	$C_{10}H_{20}Cl_4N_4O_2OsS_2$	$C_{14}H_{12}Cl_4N_4Os$	$C_{48}H_{72.5}Cl_4N_{32}O_{25.25}Os$
fw	468.16	568.28	624.42	568.28	1833.88
space group	$P\bar{1}$	$P2_1/c$	$P2_1/c$	$P2_1/c$	$Pca2_1$
a [Å]	6.5110(4)	9.925(3)	9.2546(3)	9.8508(3)	31.5673(9)
b [Å]	7.1695(5)	12.022(3)	14.6087(5)	12.1309(4)	16.9392(6)
c [Å]	7.4983(5)	6.9802(15)	7.6323(3)	6.9496(2)	14.3896(5)
α [deg]	115.562(4)				
β [deg]	110.932(4)	108.128(11)	99.294(2)	108.036(2)	
γ [deg]	92.719(4)				
V [Å^3]	286.36(3)	791.5(3)	1018.32(6)	789.66(4)	7694.5(4)
Z	1	2	2	2	4
λ [Å]	0.71073	0.71073	0.71073	0.71073	0.71073
ρ_{calcd} [g cm^{-3}]	2.715	2.384	2.036	2.390	1.583
crystal size [mm^3]	0.20 × 0.06 × 0.04	0.20 × 0.06 × 0.01	0.50 × 0.25 × 0.03	0.44 × 0.20 × 0.02	0.20 × 0.18 × 0.04
T [K]	100	100	100	100	100
μ [mm^{-1}]	12.035	8.732	7.001	8.753	1.890
R_1[a]	0.0237	0.0313	0.0205	0.0184	0.0486
wR_2[b]	0.0552	0.0729	0.0462	0.0450	0.1310
GOF[c]	1.071	0.949	1.067	1.090	1.050

[a] $R_1 = \Sigma||F_o| - |F_c||/\Sigma|F_o|$. [b] $wR_2 = \{\Sigma w(F_o^2 - F_c^2)^2/\Sigma w(F_o^2)^2\}^{1/2}$. [c] GOF = $\{\Sigma[w(F_o^2 - F_c^2)^2]/(n-p)\}^{1/2}$, where n is the number of reflections and p is the total number of parameters refined.

Found: C, 29.64; H, 1.90; N, 9.68. ESI-MS in MeOH (negative): m/z 331 $[OsCl_4]^-$, 448 $[OsCl_4(Hbzim)-H]^-$, 567 $[OsCl_4(Hbzim)_2-H]^-$. MIR, cm^{-1}: 591, 658, 689, 733, 775, 988, 1117, 1246, 1422, 1490, 1945, 2018, 2150, 2189, 2235, 2364, and 3338. FIR, cm^{-1}: 161, 320, 349, 643. UV−vis (DMSO), λ_{max}, nm (ε, M^{-1} cm^{-1}): 354 sh (6318), 373 (6176), 454 (3362), 513 (4075). ^{1}H NMR (DMSO-d_6, 500.32 MHz): δ −5.58 (s, 1H, H_2), 4.58 (d, 1H, J = 8.17 Hz, $H_{4\ or\ 7}$), 5.55 (t, 1H, J = 7.27 Hz, $H_{5\ or\ 6}$), 6.71 (d, 1H, J = 8.18 Hz, $H_{4\ or\ 7}$), 6.74 (t, 1H, J = 7.26 Hz, $H_{5\ or\ 6}$), 9.00 (s, 1H, H_1) ppm. ^{13}C{^{1}H} NMR (DMSO-d_6, 125.81 MHz): δ 114.64 ($C_{8\ or\ 9}$), 122.64 {6.71} ($C_{4\ or\ 7}$), 127.45 {6.74} ($C_{5\ or\ 6}$), 133.73 {4.58} ($C_{4\ or\ 7}$), 135.48 {5.55} ($C_{5\ or\ 6}$), 159.43 ($C_{8\ or\ 9}$), 200.46 (C_2) ppm. Suitable crystals for X-ray diffraction study were grown from a solution of **4** in DMSO.

*trans-[$OsCl_4$(Hpz)$_2$]·cucurbit[7]uril·11.25H_2O (**5**·11.25H_2O).* A suspension of **1** (4 mg, 0.009 mmol) and cucurbit[7]uril (10 mg, 0.009 mmol) in water (3 mL) was heated at 100 °C for 2.5 h in a closed Schlenk vial. The hot solution was filtered. Suitable crystals of **5**·11.25H_2O for X-ray diffraction study were grown from the filtrate at room temperature over 24 h.

Physical Measurements. Elemental analyses were performed by the Microanalytical Laboratory of the Faculty of Chemistry of the University of Vienna. MIR spectra were obtained by using an ATR unit with a Perkin-Elmer 370 FTIR 2000 instrument (4000−400 cm^{-1}). FIR spectra were recorded on the same instrument in transmission mode using CsI pellets. UV−vis spectra were recorded on a Perkin-Elmer Lambda 20 UV−vis spectrophotometer using samples dissolved in DMSO, DMF, methanol, or water containing 1% DMSO. Electrospray ionization mass spectrometry was carried out with a Bruker Esquire 3000 instrument (Bruker Daltonics, Bremen, Germany) by using methanol as solvent. Electron impact mass spectrometry was carried out on a Finnigan MAT95 mass spectrometer. Expected and measured isotope distributions were compared. Cyclic voltammogramms were measured in a three-electrode cell using a 2 mm diameter glassy carbon disk working electrode, a platinum auxiliary electrode, and an Ag|Ag$^+$ reference electrode containing 0.1 M $AgNO_3$. Measurements were performed at room temperature using a EG&G PARC potentiostat/galvanostat model 273A. Deareation of solutions was accomplished by passing a stream of argon through the solution for 5 min prior to the measurement and then maintaining a blanket atmosphere of argon over the solution during the measurement. The potentials were measured in 0.2 M (n-Bu_4N)[BF_4]/DMSO using [Fe(η^5-C_5H_5)$_2$] ($E_{1/2}^{ox}$ = +0.68 V vs NHE)[18] as internal standard and are quoted relative to NHE. Thermogravimetry was performed under nitrogen atmosphere on a Mettler Toledo TGA/SDTA851 instrument. The ^{1}H, ^{13}C and ^{15}N NMR spectra were recorded at 500.32, 125.81, and 50.69 MHz on a Bruker DPX500 (Ultrashield Magnet) in DMSO-d_6. 2D ^{13}C,^{1}H HSQC, ^{15}N,^{1}H HSQC, ^{13}C,^{1}H HMBC and ^{1}H,^{1}H COSY experiments were performed for **1**, **3**, and **4**, while a homonuclear decoupling experiment only for **1**.

Crystallographic Structure Determination. X-ray diffraction measurements were performed on a Bruker X8 APEXII CCD diffractometer. Single crystals were positioned at 35, 35, 40, 40, and 50 mm from the detector, and 1150, 1200, 3557, 1758, and 1569 frames were measured, each for 30, 80, 20, 30, and 60 s over 1° scan width for **1**, **2**, **3**·2DMSO, **4**, and **5**·11.25H_2O, correspondingly. The data were processed using the SAINT software.[19] The structures were solved by direct methods and refined by full-matrix least-squares techniques. Non-H atoms were refined with anisotropic displacement parameters. H atoms were inserted in calculated positions and refined with a riding model. The following software programs and computer were used: structure solution, SHELXS-97;[20] refinement, SHELXL-97;[21] molecular diagrams, ORTEP-3;[22] computer, Intel CoreDuo. Crystal data, data collection parameters, and structure refinement details for **1**, **2**, **3**·2DMSO, **4**, and **5**·11.25H_2O are given in Table 1.

Cell Lines and Culture Conditions. CH1 (ovarian carcinoma, human) cells were a gift from Lloyd R. Kelland (CRC Centre for Cancer Therapeutics, Institute of Cancer Research, Sutton, U.K.). A549 (nonsmall cell lung cancer, human) and SW480 (colon carcinoma, human) cells were kindly provided by Brigitte Marian (Institute of Cancer Research, Department of Medicine I, Medical University of Vienna, Austria). Cells were grown in 75 cm^2 culture flasks (Iwaki/Asahi Technoglass) as adherent monolayer cultures in Minimal Essential

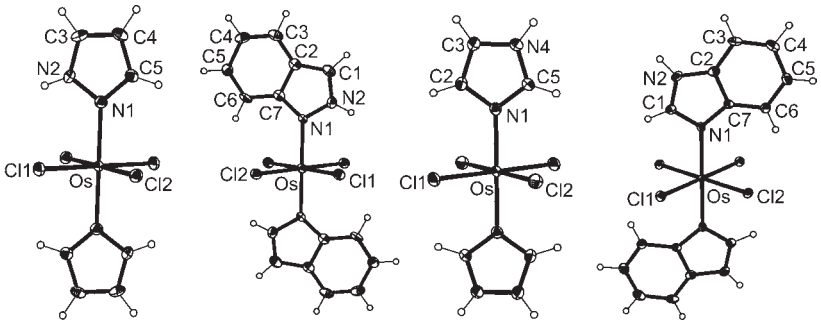

Figure 1. ORTEP view of $[Os^{IV}Cl_4(Hpz)_2]$ (**1**), $[Os^{IV}Cl_4(Hind)_2]$ (**2**), $[Os^{IV}Cl_4(Him)_2]$ in **3**·2DMSO, and $[Os^{IV}Cl_4(Hbzim)_2]$ (**4**). Thermal ellipsoids are drawn at 50% probability level.

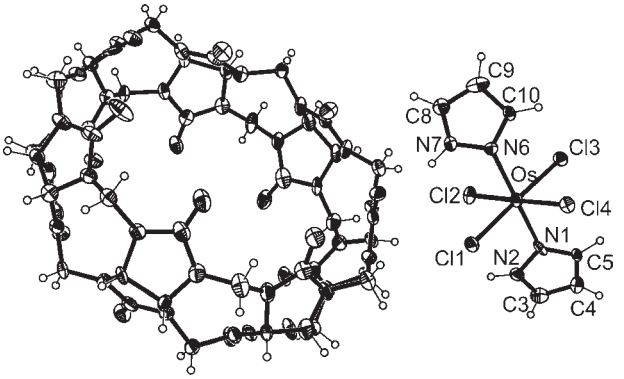

Figure 2. ORTEP view of *trans*-$[Os^{IV}Cl_4(Hpz)_2]$·cucurbit[7]uril in **5**·11.25H_2O. Thermal ellipsoids are drawn at 50% probability level.

Medium (MEM) supplemented with 10% heat-inactivated fetal bovine serum, 1 mM sodium pyruvate, and 2 mM L-glutamine (all purchased from Sigma-Aldrich) without antibiotics. Cultures were maintained at 37 °C in a humidified atmosphere containing 5% CO_2 and 95% air.

Cytotoxicity in Cancer Cell Lines. Cytotoxicity in the cell lines mentioned above was determined by the colorimetric MTT assay (MTT = 3-(4,5-dimethyl-2-thiazolyl)-2,5-diphenyl-2*H*-tetrazolium bromide, purchased from Fluka). For this purpose, cells were harvested from culture flasks by trypsinization and seeded in 100 μL/well aliquots in MEM supplemented with 10% heat-inactivated fetal bovine serum, 1 mM sodium pyruvate, 4 mM L-glutamine, and 1% nonessential amino acids (100 × stock solution) into 96-well microculture plates (Iwaki/Asahi Technoglass) in the following densities to ensure exponential growth of untreated controls throughout the experiment: 1.5×10^3 (CH1), 4.0×10^3 (A549), and 2.5×10^3 (SW480) viable cells per well. Cells were allowed to settle and resume proliferation for 24 h and were then exposed to the test compounds by addition of 100 μL/well aliquots of appropriate dilutions in the same medium. For this purpose, compounds were dissolved in DMSO first and diluted in medium such that the effective DMSO content did not exceed 0.5% whenever necessary. After exposure for 96 h, the medium was replaced by 100 μL/well RPMI 1640 medium (supplemented with 10% heat-inactivated fetal bovine serum and 4 mM L-glutamine) plus 20 μL/well solution of MTT in phosphate-buffered saline (5 mg/mL) (all purchased from Sigma-Aldrich). After incubation for 4 h, medium/MTT mixtures were removed, and the formazan precipitate formed by viable cells was dissolved in DMSO (150 μL/well). Optical densities at 550 nm (corrected for unspecific absorbance at 690 nm) were measured with a microplate reader (Tecan Spectra Classic) to yield relative quantities of viable cells as percentage of untreated controls, and 50% inhibitory concentrations (IC_{50}) were calculated by interpolation. Evaluation is based on at least two (in case of inactivity) or three independent experiments, each comprising triplicate samples.

RESULTS AND DISCUSSION

Synthesis. By exploring further the Anderson type rearrangement reactions, which already enabled the synthesis of (azole)pentachloridoosmate(IV) complexes,[5] we obtained *trans*-bis(azole)-tetrachloridoosmium(IV) complexes following the reaction scheme:

$$(H_2azole)_2[Os^{IV}Cl_6] \xrightarrow[-HCl]{} (H_2azole)[Os^{IV}Cl_5(Hazole)] \xrightarrow[-HCl]{} [Os^{IV}Cl_4(Hazole)_2]$$

The reactions were performed in suspensions of the starting compounds $(H_2azole)_2[Os^{IV}Cl_6]$, where Hazole = 1*H*-pyrazole, 1*H*-imidazole, and 1*H*-benzimidazole, in 1-hexanol at 160 °C to yield **1**, **3**, and **4**. The indazole product **2** was obtained by heating the indazolium hexachloridoosmate(IV) in the solid state at 150 °C. The liberation of two molecules of hydrochloric acid was followed by thermogravimetric analysis and the formation of bis-azole complexes by NMR spectroscopy. The *trans*-$[Os^{IV}Cl_4(Hazole)_2]$ complexes can also be prepared starting from $(H_2azole)[Os^{IV}Cl_5(Hazole)]$ providing further evidence for Anderson type rearrangement reaction in the solid state (Supporting Information, Figure S1). The complexes **1**−**4** were synthesized in yields ranging from 19 to 82%. It is worth noting that in the case of indazole the only product isolated was *trans*-$[Os^{IV}Cl_4(2H\text{-ind})_2]$. All four compounds are nonelectrolytes and hence show poor solubility in aqueous media. Therefore, attempts to encapsulate them in a cucurbit[7]uril host molecule to improve the aqueous solubility and use the latter as a vehicle for drug delivery [23] to the cell, as reported for platinum [24,25] and metallocene[26] anticancer agents, have been undertaken. However, instead of inclusion complexes adduct **5** resulted from reaction of **1** with cucurbit[7]uril, as described for other metal chlorido complexes. [27−30]

Crystal Structures. The results of X-ray diffraction studies of complexes **1**, **2**, **3**·2DMSO, **4**, and **5**·11.25H_2O are shown in Figures 1 and 2, respectively. Selected bond lengths and angles are quoted in Table 2. To our knowledge **1**−**4** are the first bis(azole)tetrachloridoosmium(IV) complexes characterized by X-ray crystallography as individual compounds.

Complex **1** crystallized in the triclinic centrosymmetric space group $P\bar{1}$, while compounds **2**, **3**·2DMSO, and **4** crystallized in the monoclinic space group $P2_1/c$. There is one molecule of **1**

dx.doi.org/10.1021/ic200728b |*Inorg. Chem.* 2011, 50, 7690–7697

Table 2. Selected Bond Lengths (Å) and Angles (deg) in the Coordination Polyhedron of Osmium(IV) in 1−4

	1	2	3·2DMSO	4
		Atom1−Atom2		
Os−N1	2.059(5)	2.050(5)	2.069(2)	2.073(2)
Os−Cl1	2.3301(14)	2.3439(16)	2.3381(6)	2.3250(7)
Os−Cl2	2.3326(14)	2.3395(15)	2.3139(6)	2.3280(7)
		Atom1−Atom2−Atom3		
Cl1−Os−Cl2	90.58(5)	90.22(6)	89.67(2)	88.75(3)
N1−Os−Cl1	90.03(14)	91.73(15)	90.34(6)	90.47(7)
N1−Os−Cl2	89.16(14)	89.32(15)	89.41(6)	90.13(7)

and two molecules of **2**−**4** in the corresponding unit cells. In addition, complex **3** contains one molecule of cocrystallized DMSO per asymmetric unit. The osmium ion in all four complexes lies on a center of symmetry, and the centrosymmetric molecules are of point group symmetry C_i. The osmium atom displays distorted octahedral coordination geometry with four chlorido ligands in the equatorial positions and two azole ligands bound axially. Comparison of the bond lengths in the coordination environment of osmium in **1**−**4** shows (Table 2) that the longer the axial bonds, the shorter are the equatorial ones.

Both *trans*-azole ligands in **1**−**4** lie in one plane in contrast to what was found in $(Ph_4P)[trans\text{-}Ru^{III}Cl_4(1H\text{-ind})_2]$, where the 1*H*-indazole ligands are significantly twisted.[31] The plane through both azole ligands crosses the equatorial plane between chloride ligands, the torsion angles $\Theta_{Cl1-Os-N1-N2}$, $\Theta_{Cl2-Os-N2-N1}$, $\Theta_{Cl1-Os-N1-C2}$, and $\Theta_{Cl1-Os-N1-C1}$ being −30.4(4), −33.2(6), −31.6(2), and −47.8(2)°, respectively.

Of particular interest is the structure of indazole derivative **2** (Figure 1), in which the indazole is stabilized in a quinoid tautomeric form coordinating to osmium via nitrogen atom N1. This mode of coordination has not been documented for any transition metal yet. Indazole acts mainly as a monodentate neutral ligand in metal complexes binding to metal ions via N2. In a few cases, it was found to be deprotonated, acting as a bridging ligand in polynuclear metal complexes[32] or even more rarely as a monodentate indazolate ligand coordinated via N1 or N2.[3e,33]

The molecules of **1** in the crystal structure form a chain running almost parallel to axis *a* (Supporting Information, Figure S2). Hydrogen bonding interactions between the pyrazole nitrogen atom N2 as a proton donor and chloride ligand $Cl2^i$ as a proton acceptor are evident [N2···$Cl2^i$ 3.270, N2−H 0.88, H···$Cl2^i$ 2.511 Å, N2−H···$Cl2^i$ 144.86°; symmetry code i: $x-1, y, z$]. The unit cell packing diagram for **2** is shown in Supporting Information, Figure S3. A bifurcated hydrogen bond between N2 as proton donor and chloride ligands $Cl1^i$ and $Cl2^{ii}$ as proton acceptors is present in the crystal structure [N2···$Cl1^i$ 3.444, N2···$Cl2^{ii}$ 3.143 Å]. In addition, stacking interaction between indazole ligands of neighboring molecules of **2** is also evident. The interplanar separation is about 3.4 Å (Supporting Information, Figure S4). Intermolecular hydrogen bonding interaction between the imidazole nitrogen N4 and the oxygen atom $O1^i$ (2.698 Å) of cocrystallized DMSO is shown in Supporting Information, Figure S5. A bifurcated hydrogen bonding interaction between atom N2 of benzimidazole ligand in one molecule with chloride ligands $Cl1^i$ and $Cl2^{ii}$ of two adjacent molecules of **4** [N2···$Cl1^i$ 3.541, N2···$Cl2^{ii}$ 3.504 Å], along with $\pi-\pi^*$ stacking interactions between heteroaromatic rings separated at about 3.4 Å are displayed in Supporting Information, Figure S6.

In contrast to **1**−**4**, *trans*-$[Os^{IV}Cl_4(Hpz)_2]\cdot$cucurbit[7]uril (**5**·11.25H_2O) crystallizes in a noncentrosymmetric orthorhombic space group $Pca2_1$. The result of X-ray diffraction study of this complex is shown in Figure 2. The bond lengths Os−N1 and Os−N6 of 2.076(7) and 2.077(7) Å, respectively, along with Os−Cl1, Os−Cl2, Os−Cl3, and Os−Cl4 [2.386(2), 2.357(2), 2.382(2) and 2.386(2), correspondingly] are significantly longer than the Os−N1, Os−Cl1, and Os−Cl2 bond lengths in **1** (Table 2). The atom N2 is involved in a hydrogen bond N2−H···$Cl3^i$ with the following geometrical parameters: N2···$Cl3^i$ 3.242 Å, N2−H···$Cl3^i$ 133.6°, while atom N7 forms a hydrogen bond with a cocrystallized water molecule [N7···O11 2.899 Å, N7−H···O11 133.6°].

Passage of *trans*-$[Os^{IV}Cl_4(Hpz)_2]$ through the portal of cucurbit[7]uril could experience strong repulsive forces at distances less than the sums of van der Waals radii (portal diameter 5.4 Å,[23] cavity width 7.3 Å,[23] and Cl2···Cl4 vector in **5** of 4.74 Å). Although the cucurbit[7]uril does form an inclusion complex with a metal halide, namely, *cis*-$[SnCl_4(H_2O)_2]$, a more sophisticated mechanism of portal passage and formation of the complex was suggested.[34] First a tetrahedral $SnCl_4$ molecule enters the host molecule, which then undergoes hydration. Partial inclusion of oxaliplatin into cucurbit[7]uril has been also reported.[35]

NMR Spectra. The ^1H, ^{13}C and ^{15}N NMR spectra show signals due to coordinated azole heterocycles (**1**−**4**). The assignment of the protons and carbon atoms of the azole heterocycle is in some cases hindered by the temperature-independent paramagnetism of low-spin d^4 osmium(IV) which causes some broadening of the signals and large shifts relative to uncoordinated azoles at room temperature. Protons close to the metal center generally show larger shifts to negative values. However, it should be noted that signals are remarkably sharp for the majority of the compounds studied. We succeeded to obtain two-dimensional NMR spectra for the compounds **1**, **3**, and **4** ($^{13}C,^1H$ HSQC, $^{15}N,^1H$ HSQC (**1**, **3**), $^{13}C,^1H$ HMBC, $^1H,^1H$ COSY).

trans-[OsCl$_4$(Hpz)$_2$]. The H_1 proton in **1** at 19.21 ppm was identified from the $^{15}N,^1H$ HSQC plot with a chemical shift for N_1 at 115.50 ppm. Because of the C_s local symmetry of the coordinated pyrazole, the H_3 and H_5 signals do not overlap as is the case for the metal-free pyrazole. The resonance signal H_5 is observed as a singlet at −2.97 ppm, while H_3 is observed as a doublet at −5.59 ppm. The assignment of the H_3 and H_5 signals was enabled by a homonuclear decoupling experiment. H_4 shows a broad signal at 6.48 ppm. In the $^{13}C\{^1H\}$ NMR spectra of **1** the carbon resonances of C_4, C_5, and C_3 appear at 73.52, 181.14, and 218.41 ppm, respectively.

trans-[OsCl$_4$(Him)$_2$]. The H_1 proton in **3** at 12.29 ppm was identified from the $^{15}N,^1H$ HSQC plot with the chemical shift for N_1 at 157.08 ppm. The H_4 and H_5 resonances do not overlap as is the case for the metal-free imidazole. The singlets at −0.51, 7.29, and 7.86 ppm were attributed to H_2, H_4, or H_5; a more precise assignment failed. The corresponding carbon resonances of C_2, C_4, and C_5 were found at 119.52 {7.29}, 114.45 {7.86}, and 188.36 {−0.51} ppm. The $^{13}C,^1H$ HMBC plot does not enable the assignment of C_2, C_4, C_5 and H_2, H_4, H_5 because of the same number of cross peaks.

trans-[OsCl$_4$(Hbzim)$_2$]. Compound **4** shows two singlets, two doublets, and two triplets in the ^1H NMR spectrum. The H_1

dx.doi.org/10.1021/ic200728b |*Inorg. Chem.* 2011, 50, 7690–7697

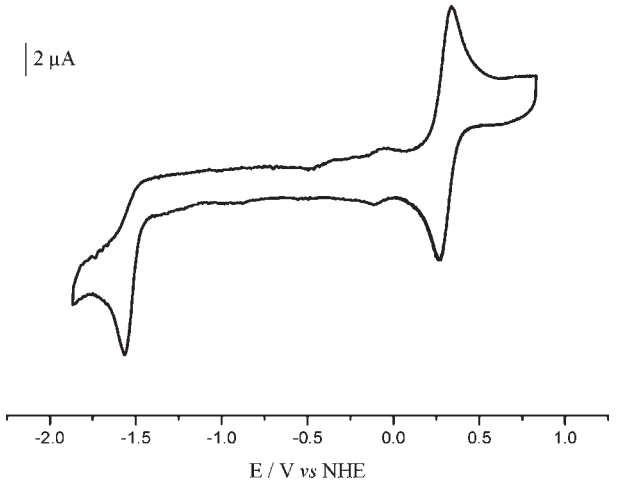

Figure 3. Cyclic voltammogram of 0.2 M solution of **3** in DMSO at a carbon disk working electrode at a scan rate of 0.2 V/s, starting the scan in cathodic direction.

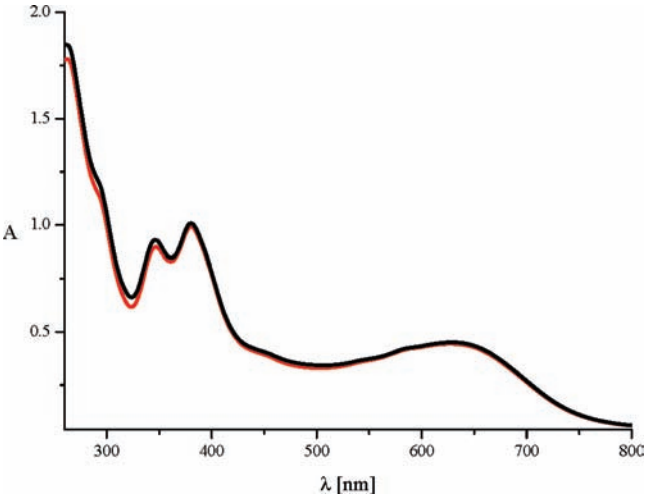

Figure 4. UV−vis spectra of an aqueous solution (containing 1% DMSO) of **4**, measured immediately after dissolution and 24 h thereafter.

Table 3. Cyclic Voltammetric Data for 1−4

complex	E_p Os(III/II)	E_{calc}	$E_{1/2}$ Os(IV/III)[a], (ΔE_p)[b]
1	−1.22	−0.97	0.50 (68)
2	−1.17	−1.01	0.42 (69)
3	−1.55	−1.19	0.31 (68)
4	−1.41	−1.17	0.37 (71)

[a] Potentials $E_{1/2}$ ($E_{1/2} = (E_{pa} + E_{pc})/2$, where E_{pa} and E_{pc} are the anodic and cathodic peak potentials) are given in V and measured at a scan rate of 0.2 V/s in DMSO, using ferrocene as internal standard, and are quoted relative to NHE. [b] ΔE_p values ($\Delta E_p = E_{pa} - E_{pc}$) are given in mV.

proton is found as a singlet at 9.00 ppm, while a strongly shifted singlet at −5.58 ppm was assigned to H_2, which is in close proximity to the coordination site. The two doublets were attributed to H_4 and H_7, whereas the two triplets to H_5 and H_6. In the $^{13}C\{^1H\}$ NMR spectra the carbon resonances of C_4 and C_7 are seen at 122.64 {6.71} and 133.73 {4.58} ppm, while those for C_5, C_6 at 127.45 {6.74}, 135.48 {5.55} and C_2 at 200.46 ppm, respectively. There are two signals at 114.64 and 159.43 ppm for the quarternary carbons C_8 and C_9. Neither the $^{13}C,^1H$ HMBC nor the $^1H,^1H$ COSY allowed to differentiate between H_4/H_7 (C_4/C_7) and H_5/H_6 (C_5/C_6).

Electrochemical Behavior. The cyclic voltammograms (CVs) of the complexes **1**−**4** in DMSO (0.2 M (n-Bu_4N)-[BF_4]/DMSO) at a carbon disk working electrode, recorded with a scan rate of 0.2 V/s, display a reversible one-electron reduction wave attributed to the $Os^{IV} \rightarrow Os^{III}$ process with potential values ranging from 0.31 to 0.50 V and an irreversible single electron reduction wave (I^{red}) attributed to the $Os^{III} \rightarrow Os^{II}$ process with E_p potential values between −1.17 and −1.55 V versus NHE (Figure 3, Table 3). The redox waves Os^{IV}/Os^{III} are characterized by a peak-to-peak separation (ΔE_p) of 68−71 mV and an anodic peak current (i_{pa}) that is almost equal to the cathodic peak current (i_{pc}), as expected for reversible electron transfer processes. The one-electron nature of these processes was verified by comparing the peak current height (i_p) with that of standard ferrocene/ferrocenium couples under identical experimental conditions. The reduction potentials Os^{IV}/Os^{III} are

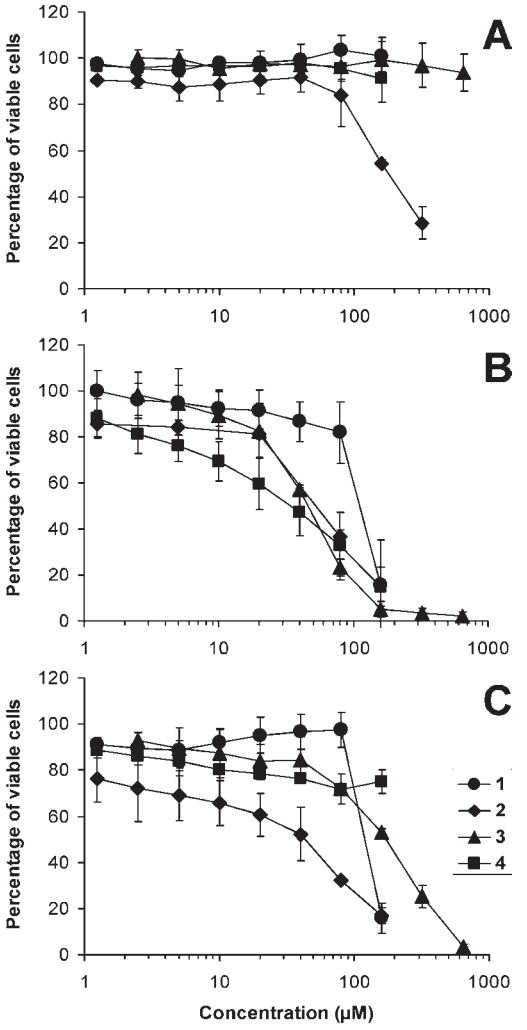

Figure 5. Concentration−effect curves of compounds **1**−**4** in (A) A549, (B) CH1, and (C) SW480 cells, obtained by the MTT assay (96 h exposure).

in the following order: $E_{1/2}(\mathbf{1}) > E_{1/2}(\mathbf{2}) > E_{1/2}(\mathbf{4}) > E_{1/2}(\mathbf{3})$, which agrees quite well with the relative electron-donating

dx.doi.org/10.1021/ic200728b |Inorg. Chem. 2011, 50, 7690–7697

Table 4. Cytotoxicity of Compounds 1−4 and the Reference Compound KP1019 in Three Human Cancer Cell Lines

	IC_{50}, μM[a]		
compound	A549	CH1	SW480
1	>160	115 ± 14	120 ± 5
2	181 ± 11	53 ± 4	41 ± 14
3	>640	46 ± 1	173 ± 9
4	>160	36 ± 16	>160
KP1019		44 ± 11[b]	79 ± 5[b]

[a] 50% inhibitory concentrations (means ± standard deviations from at least three independent experiments), as obtained by the MTT assay (exposure time: 96 h). [b] C. Bartel, M. A. Jakupec, unpublished results.

character of the azole ligands [E_L(Hpz) > E_L(2*H*-ind) > E_L(Hbzim) > E_L(Him)].[36,37] The reduction potential for $Os^{III} \rightarrow Os^{II}$ was calculated using Lever's equation[38] (eq 1) [E_L(Cl) = −0.24,[37] E_L(2*H*-ind) = 0.18,[39] E_L(Hpz) = 0.20,[37] E_L(Hbzim) = 0.1,[37] E_L(Him) = 0.09,[40] $S_M(Os^{III}/Os^{II})$ = 1.01,[37] $I_M(Os^{III}/Os^{II})$ = −0.40[37]].

$$E = S_M \cdot \sum E_L + I_M \quad (1)$$

The values of E_{calc} for Os^{III}/Os^{II} obtained by using this formula are quoted for comparison with the E_p values measured for Os^{III}/Os^{II} in Table 3.

Aqueous Solubility and Resistance to Hydrolysis. The solubility of the complexes **1**−**4** in water containing 1% DMSO at 298 K varies from 1.9 (**1** and **3**) to 2.1 mM (**4**). The complexes remain intact in this medium for at least 24 h as is shown for complex **4** in Figure 4 by UV−vis spectroscopy. The optical spectra of **1**−**4** in DMSO are shown in Supporting Information, Figure S7.

Cytotoxicity in Cancer Cell Lines. The cytotoxicity of compounds **1**−**4** was assessed by means of the MTT assay in three human cell lines originating from different malignant tumors. A 96 h exposure yielded the concentration−effect curves depicted in Figure 5 and IC_{50} values listed in Table 4. IC_{50} values are mostly in the 10^{-5} M range in the rather chemosensitive ovarian cancer cell line CH1, but mostly higher than 100 μM or even higher than the maximally applicable concentrations (because of limited solubility) in the less chemosensitive colon cancer (SW480) and nonsmall cell lung cancer (A549) cells. Best of the four compounds, the indazole complex **2** retains cytotoxic properties in those two cell lines. The cytotoxicity of this compound is in a range well comparable with that of the clinically studied ruthenium complex $(H_2ind)[Ru^{III}Cl_4(Hind)_2]$ (KP1019).[12] Furthermore, this compound is similarly potent as or up to 2.4 times more potent than the corresponding monoindazole complex $(H_2ind)[Os^{IV}Cl_5(2H\text{-ind})]$, depending on the cell line, while the cytotoxicity of the bispyrazole analogue **1** is comparable to that of the monopyrazole complex $(H_2pz)[Os^{IV}Cl_5(Hpz)]$,[5] all based on IC_{50} values. The fact that comparisons of **1**−**4** do not yield uniform structure−activity relationships in the three cell lines employed suggest that variation of the azole ligands in the compounds does not affect cytotoxic potency in a generally valid way but that the consequences for the biological effects are more complex.

Final Remarks. Anderson type transformation of $(H_2azole)_2[Os^{IV}Cl_6]$ in 1-hexanol and in the solid state resulted in complexes with the general formula *trans*-$[Os^{IV}Cl_4(Hazole)_2]$, where Hazole = 1*H*-pyrazole, 1*H*-imidazole, 2*H*-indazole, or 1*H*-benzimidazole. Comparison of the described complexes with their ruthenium analogues $(H_2azole)[Ru^{III}Cl_4(Hazole)_2]$ provides further evidence for the higher oxidation state preference of the heavier congener. Despite the nonelectrolyte character of the prepared compounds, the solubility in water containing 1% DMSO was borderline to allow the assessment of their antiproliferative activity in vitro against human cancer cell lines. An attempt to improve the solubility of the complexes by encapsulation in cucurbit[7]uril was described. The importance of this work consists in preparation of precursors, which can be suitable for the synthesis of osmium(III) analogues of KP1019, a potent investigational anticancer drug in clinical trials. In addition, a notable crystallographic contribution has been made. The complexes *trans*-$[Os^{IV}Cl_4(Hazole)_2]$ are characterized for the first time as individual compounds by X-ray crystallography. A remarkable finding is the stabilization of the quinoid-type 2*H*-indazole in **2** coordinated to metal via N1. Further attempts to prepare osmium(IV) complexes with 1*H*-indazole tautomer and inclusion complexes with cucurbit[8]uril and cucurbit[10]uril are underway in our laboratory.

■ ASSOCIATED CONTENT

Supporting Information. Thermogravimetric data for $(H_2ind)_2[OsCl_6]$ and $(H_2ind)[OsCl_5(1H\text{-ind})]$ (Figure S1), the unit cells for **1** and **2** (Figures S2, S3) as well as hydrogen bonding interactions in the crystal structures of **2**, **3**·2DMSO and **4** (Figures S4−S6), UV−vis spectra of **1**−**4** in DMSO (Figure S7). Crystallographic data for **1**, **2**, **3**·2DMSO, **4**, and **5**·11.25H_2O in CIF format. This material is available free of charge via the Internet at http://pubs.acs.org.

■ AUTHOR INFORMATION

Corresponding Author
*E-mail: vladimir.arion@univie.ac.at.

■ ACKNOWLEDGMENT

We thank Marcel Wieland, Institute of Organic Chemistry, University of Vienna, for providing us with cucurbit[7]uril, Alexander Roller for collecting the X-ray diffraction data, Prof. Dr. Markus Galanski for recording 2D NMR spectra, and Dr. Peter Unfried for thermogravimetric measurements. We are also indebted to the Austrian Science Fund (FWF) for financial support of the project I 374-N19.

■ REFERENCES

(1) (a) Allardyce, C. S.; Dorcier, A.; Scolaro, C.; Dyson, P. J. *Appl. Organomet. Chem.* **2005**, *19*, 1–10. (b) Dorcier, A.; Ang, W. H.; Bolaño, S.; Gonsalvi, L.; Juillerat-Jeannerat, L.; Laurenczy, G.; Peruzzini, M.; Phillips, A. D.; Zanobini, F.; Dyson, P. J. *Organometallics* **2006**, *25*, 4090–4096. (c) Dyson, P. J. *Chimia* **2007**, *61*, 698–703. (d) Renfrew, A. K.; Phillips, A. D.; Egger, A. E.; Hartinger, C. G.; Bosquain, S. S.; Nazarov, A. A.; Keppler, B. K.; Gonsalvi, L.; Peruzzini, M.; Dyson, P. J. *Organometallics* **2009**, *28*, 1165–1172.

(2) (a) Peacock, A. F. A.; Habtemariam, A.; Fernandez, R.; Walland, V.; Fabbiani, F. P. A.; Parsons, S.; Aird, R. E.; Jodrell, D. I.; Sadler, P. J. *J. Am. Chem. Soc.* **2006**, *128*, 1739–1748. (b) Peacock, A. F. A.; Melchart, M.; Deeth, R. J.; Habtemariam, A.; Parsons, S.; Sadler, P. J. *Chem.—Eur. J.* **2007**, *13*, 2601–2613. (c) Peacock, A. F. A.; Habtemariam, A.; Moggach, S. A.; Prescimone, A.; Parsons, S.; Sadler, P. J. *Inorg. Chem.* **2007**, *46*, 4049–4059. (d) Peacock, A. F. A.; Parsons, S.; Sadler, P. J. *J. Am. Chem. Soc.* **2007**, *129*, 3348–3357. (e) van Rijt, S. H.; Peacock,

A. F. A.; Johnstone, R. D. L.; Parsons, S.; Sadler, P. J. *Inorg. Chem.* **2009**, *48*, 1753–1752.

(3) (a) Cebrián-Losantos, B.; Krokhin, A. A.; Stepanenko, I. N.; Eichinger, R.; Jakupec, M. A.; Arion, V. B.; Keppler, B. K. *Inorg. Chem.* **2007**, *46*, 5023–5033. (b) Stepanenko, I. N.; Krokhin, A. A.; John, R. O.; Roller, A.; Arion, V. B.; Jakupec, M. A.; Keppler, B. K. *Inorg. Chem.* **2008**, *47*, 7338–7347. (c) Schmid, W. F.; John, R. O.; Arion, V. B.; Jakupec, M. A.; Keppler, B. K. *Organometallics* **2007**, *26*, 6643–6652. (d) Schmid, W. F.; John, R. O.; Mühlgassner, G.; Heffeter, P.; Jakupec, M. A.; Galanski, M.; Berger, W.; Arion, V. B.; Keppler, B. K. *J. Med. Chem.* **2007**, *50*, 6343–6355. (e) Schuecker, R.; John, R. O.; Jakupec, M. A.; Arion, V. B.; Keppler, B. K. *Organometallics* **2008**, *27*, 6587–6595.

(4) (a) Dorcier, A.; Dyson, P. J.; Gossens, C.; Rothlisberger, U.; Scopelliti, R.; Tavernelli, I. *Organometallics* **2005**, *24*, 2114–2123. (b) Dorcier, A.; Hartinger, C. J.; Scopelliti, R.; Fish, R. H.; Keppler, B. K.; Dyson, P. J. *J. Inorg. Biochem.* **2008**, *102*, 1066–1076.

(5) Büchel, G. E.; Stepanenko, I. N.; Hejl, M.; Jakupec, M. A.; Arion, V. B.; Keppler, B. K. *Inorg. Chem.* **2009**, *48*, 10737–10747.

(6) Stepanenko, I. N.; Cebrián-Losantos, B.; Arion, V. B.; Krokhin, A. A.; Nazarov, A. A.; Keppler, B. K. *Eur. J. Inorg. Chem.* **2007**, 400–411.

(7) Singh, P.; Sarkar, B.; Sieger, M.; Niemeyer, M.; Fiedler, J.; Zališ, S.; Kaim, W. *Inorg. Chem.* **2006**, *45*, 4602–4609.

(8) Peacock, A. F. A.; Sadler, P. J. *Chem.—Asian. J.* **2008**, *3*, 1890–1899.

(9) Chiorescu, I.; Stepanenko, I. N.; Arion, V. B.; Krokhin, A. A.; Keppler, B. K. The 13th International Conference on Biological Inorganic Chemistry (ICBIC XIII), Vienna, Austria, July 15−20, 2007; *J. Biol. Inorg. Chem.* (**2007**) *12* (Suppl. 1); P456, S 226.

(10) Chiorescu, I.; Stepanenko, I. N.; Arion, V. B.; Krokhin, A. A.; Scaffidi-Domianello, Y. Y.; Keppler, B. K. The 8th European Biological Chemistry Conference (EUROBIC 8), Aveiro, Portugal, July 2−7, 2006, PS7.17, p 333.

(11) Davies, J. A.; Hockensmith, C. M.; Kukushkin, V. Yu.; Kukushkin, Yu. N. *Synthetic Coordination Chemistry − Principles and Practice*; World Scientific Pub. Co.: Hackensack, NJ, 1995; pp 392−396.

(12) Jakupec, M. A.; Reisner, E.; Eichinger, A.; Pongratz, M.; Arion, V. B.; Galanski, M.; Hartinger, C. G.; Keppler, B. K. *J. Med. Chem.* **2005**, *48*, 2831–2837.

(13) Lipponer, K.-G.; Vogel, E.; Keppler, B. K. *Met.-Based Drugs* **1996**, *3*, 243–260.

(14) Smith, C. A.; Sutherland-Smith, A. J.; Kratz, F.; Baker, E. N.; Keppler, B. K. *J. Biol. Inorg. Chem.* **1996**, *1*, 424–431.

(15) Keppler, B. K.; Wehe, D.; Endres, H.; Rupp, W. *Inorg. Chem.* **1987**, *26*, 844–846.

(16) Brauer, G. *Handbuch der Präparativen Anorganischen Chemie, III*; Ferdinand Enke Verlag: Stuttgart, Germany, 1981; pp 17421744.

(17) Rudnitskaya, O. V.; Buslaeva, T. M.; Lyalina, N. N. *Zh. Neorg. Khim.* **1994**, *39*, 922–924.

(18) Barrette, W. C., Jr.; Johnson, H. W., Jr.; Sawyer, D. T. *Anal. Chem.* **1984**, *56*, 1890–1898.

(19) *SAINT-Plus, version 7.06a, and APEX2*; Bruker-Nonius AXS Inc.: Madison, WI, 2004;

(20) Sheldrick, G. M. *Acta Crystallogr.* **1990**, *A46*, 467–473.

(21) Sheldrick, G. M. *Acta Crystallogr.* **2008**, *A64*, 112–122.

(22) Johnson, G. K. Report ORNL-5138; OAK Ridge National Laboratory; Oak Ridge, TN, 1976.

(23) Isaacs, L. *Chem. Commun.* **2009**, 619–629.

(24) Wheate, B. J. *J. Inorg. Biochem.* **2008**, *102*, 2060–2066.

(25) Goldoni, L.; Grugni, M.; De Munari, S.; Cassin, M.; Bernardini, R. *Chem. Lett.* **2010**, *39*, 676–677.

(26) Buck, D. P.; Abeysinghe, P. M.; Cullinane, C.; Day, A. I.; Collins, J. G.; Harding, M. M. *Dalton Trans.* **2008**, 2328–2334.

(27) Yan, K.; Huang, Z.-Y.; Liu, S.-M.; Liang, F.; Wu, C.-T. *Wuhan Univ. J. Nat. Sci.* **2004**, *9*, 99–101.

(28) Samsonenko, D. G.; Sokolov, M. N.; Virovets, A. V.; Pervukhina, N. V.; Fedin, V. P. *Eur. J. Inorg. Chem.* **2001**, 167–172.

(29) Virovets, A. V.; Samsonenko, D. G.; Dybtsev, D. N.; Fedin, V. P.; Clegg, W. *Zhur. Strukt. Khim.* **2001**, *42*, 384–387.

(30) Virovets, A. V.; Samsonenko, D. G.; Sokolov, M. N.; Fedin, V. P. *Acta Crystallogr.* **2001**, *E57*, M33–M34.

(31) Peti, W.; Pieper, T.; Sommer, M.; Keppler, B. K.; Giester, G. *Eur. J. Inorg. Chem.* **1999**, 1551–1555.

(32) (a) Rendle, D. F.; Storr, A.; Trotter, J. *Can. J. Chem.* **1975**, *53*, 2930–2943. (b) Cortes-Llamas, S. A.; Hernández-Pérez, J. M.; Hó, M.; Munoz-Hernández, M.-A. *Organometallics* **2006**, *25*, 588–595.

(33) Fackler, J. P., Jr.; Staples, R. J.; Raptis, R. G. *Z. Kristallogr.* **1997**, *212*, 157–158.

(34) Lorenzo, S.; Day, A.; Craig, D.; Blanch, R.; Arnold, A.; Dance, I. *CrystEngComm* **2001**, *49*, 1–7.

(35) Jeon, Y. J.; Kim, S.-Y.; Ko, Y. H.; Sakamoto, S.; Yamaguchi, K.; Kim, K. *Org. Biomol. Chem.* **2005**, *3*, 2122–2125.

(36) Reisner, E.; Arion, V. B.; Keppler, B. K.; Pombeiro, A. J. L. *Inorg. Chim. Acta* **2008**, *361*, 1569–1583.

(37) Lever, A. B. P. *Inorg. Chem.* **1990**, *29*, 1271–1285.

(38) Lever, A. B. P.: Dodsworth, E. S. *Inorganic Electronic Structure and Spectroscopy*; Wiley: New York, 1999; pp 277−290.

(39) Büchel, G. E.; Stepanenko, I. N.; Heffeter, P.; Hejl, M.; Jakupec, M. A.; Keppler, B. K.; Berger, W. E.; Arion, V. B. manuscript in preparation.

(40) Reisner, E.; Arion, V. B.; Eichinger, A.; Kandler, N.; Giester, G.; Pombeiro, J. A. L.; Keppler, B. K. *Inorg. Chem.* **2005**, *44*, 6704–6716.